Research Article | Vol. 26, No. 15 | 23 Jul 2018 | OPTICS EXPRESS 19115
Optics EXPRESS

# Cavity optofluidics: a μdroplet's whispering-gallery mode makes a μvortex

DANIEL BAR-DAVID,* SHAI MAAYANI, LEOPOLDO L. MARTIN, AND TAL CARMON

*Department of Mechanical Engineering, Technion-Israel Institute of Technology, Haifa 32000, Israel*
**danielba@technion.ac.il*

**Abstract:** We experimentally demonstrate light-flow interaction, in which the angular momentum of circulating light excites micro-vortices. In contrast with the solid-phase of matter, where one has to overcome static friction in order to start motion, liquids have no "static drag." Relevant to almost all optofluidic micro-systems hence, μWatt optical power is sufficient to start flows, even in liquids 50 times more viscous than water. We map the flows to be three-dimensional (3D) by using a technique based on fluorescent nano-emitters; to reveal, as expected, flow speeds proportional to power divided by viscosity.



**OCIS codes:** (140.4780) Optical resonators; (140.3945) Microcavities.

## References and links

1. F. Vollmer and S. Arnold, "Whispering-gallery-mode biosensing: Label-free detection down to single molecules," Nat. Methods **5**(7), 591–596 (2008).
2. C. Y. Fainman, L. Lee, D. Psaltis, and C. Yang, *Optofluidics : Fundamentals, Devices, and Applications* (McGraw-Hill, 2009).
3. X. Fan and I. M. White, "Optofluidic microsystems for chemical and biological analysis," Nat. Photonics **5**(10), 591–597 (2011).
4. F. Vollmer and L. Yang, "Label-free detection with high-Q microcavities: a review of biosensing mechanisms for integrated devices," Nanophotonics **1**(3-4), 267–291 (2012).
5. S. Arnold, M. Khoshsima, I. Teraoka, S. Holler, and F. Vollmer, "Shift of whispering-gallery modes in microspheres by protein adsorption," Opt. Lett. **28**(4), 272–274 (2003).
6. G. Yang, I. M. White, and X. Fan, "An opto-fluidic ring resonator biosensor for the detection of organophosphorus pesticides," Sens. Actuators B Chem. **133**(1), 105–112 (2008).
7. T. Lu, H. Lee, T. Chen, S. Herchak, J.-H. Kim, S. E. Fraser, R. C. Flagan, and K. Vahala, "High sensitivity nanoparticle detection using optical microcavities," Proc. Natl. Acad. Sci. U.S.A. **108**(15), 5976–5979 (2011).
8. L. He, Ş. K. Özdemir, J. Zhu, W. Kim, and L. Yang, "Detecting single viruses and nanoparticles using whispering gallery microlasers," Nat. Nanotechnol. **6**(7), 428–432 (2011).
9. A. M. Armani, D. K. Armani, B. Min, K. J. Vahala, and S. M. Spillane, "Ultra-high-Q microcavity operation in H2O and D2O," Appl. Phys. Lett. **87**(15), 151118 (2005).
10. M. Sumetsky, Y. Dulashko, and R. S. Windeler, "Optical microbubble resonator," Opt. Lett. **35**(7), 898–900 (2010).
11. K. Hyun Kim, G. Bahl, W. Lee, J. Liu, M. Tomes, X. Fan, and T. Carmon, "Cavity optomechanics on a microfluidic resonator with water and viscous liquids," Light Sci. Appl. **2**(11), 110 (2013).
12. A. Watkins, J. Ward, Y. Wu, and S. N. Chormaic, "Single-input spherical microbubble resonator," Opt. Lett. **36**(11), 2113–2115 (2011).
13. A. Ashkin and J. M. Dziedzic, "Observation of Resonances in the Radiation Pressure on Dielectric Spheres," Phys. Rev. Lett. **38**(23), 1351–1354 (1977).
14. J. B. Snow, S.-X. Qian, and R. K. Chang, "Stimulated Raman scattering from individual water and ethanol droplets at morphology-dependent resonances," Opt. Lett. **10**(1), 37–39 (1985).
15. M. Hossein-Zadeh and K. J. Vahala, "Fiber-taper coupling to Whispering-Gallery modes of fluidic resonators embedded in a liquid medium," Opt. Express **14**(22), 10800–10810 (2006).
16. A. Jonáš, Y. Karadag, M. Mestre, and A. Kiraz, "Probing of ultrahigh optical Q-factors of individual liquid microdroplets on superhydrophobic surfaces using tapered optical fiber waveguides," J. Opt. Soc. Am. B **29**(12), 3240 (2012).
17. S. Kaminski, L. L. Martin, and T. Carmon, "Tweezers controlled resonator," Opt. Express **23**(22), 28914–28919 (2015).
18. R. Zullo, A. Giorgini, S. Avino, P. Malara, P. De Natale, and G. Gagliardi, "Laser-frequency locking to a whispering-gallery-mode cavity by spatial interference of scattered light," Opt. Lett. **41**(3), 650–652 (2016).
19. S. Maayani, L. L. Martin, and T. Carmon, "Water-walled microfluidics for high-optical finesse cavities," Nat. Commun. **7**, 10435 (2016).

#332673 https://doi.org/10.1364/OE.26.019115
Journal © 2018 Received 29 May 2018; accepted 28 Jun 2018; published 12 Jul 2018

Optics EXPRESS

20. S. T. Attar, V. Shuvayev, L. Deych, L. L. Martin, and T. Carmon, "Level-crossing and modal structure in microdroplet resonators," Opt. Express **24**(12), 13134–13141 (2016).
21. R. Dahan, L. L. Martin, and T. Carmon, "Droplet optomechanics," Optica **3**(2), 175 (2016).
22. S. Kaminski, L. L. Martin, S. Maayani, and T. Carmon, "Ripplon laser through stimulated emission mediated by water waves," Nat. Photonics **10**(12), 758–761 (2016).
23. S. Maayani, L. L. Martin, S. Kaminski, and T. Carmon, "Cavity optocapillaries," Optica **3**(5), 552 (2016).
24. S. Arnold, D. Keng, S. I. Shopova, S. Holler, W. Zurawsky, and F. Vollmer, "Whispering gallery mode Carousel-a photonic mechanism for enhanced nanoparticle detection in biosensing," Opt. Express **17**(8), 6230–6238 (2009).
25. A. Matsko, *Practical Applications of Microresonators in Optics and Photonics* (CRC Press, 2010), p. 588.
26. L. A. Weinstein, *Open Resonators and Open Waveguides* (Golem Press, 1969).
27. M. Tomes, K. J. Vahala, and T. Carmon, "Direct imaging of tunneling from a potential well," Opt. Express **17**(21), 19160–19165 (2009).
28. J. C. Knight, G. Cheung, F. Jacques, and T. A. Birks, "Phase-matched excitation of whispering-gallery-mode resonances by a fiber taper," Opt. Lett. **22**(15), 1129–1131 (1997).
29. M. Cai, O. Painter, and K. J. Vahala, "Observation of Critical Coupling in a Fiber Taper to a Silica-Microsphere Whispering-Gallery Mode System," Phys. Rev. Lett. **85**(1), 74–77 (2000).
30. S. M. Spillane, T. J. Kippenberg, O. J. Painter, and K. J. Vahala, "Ideality in a Fiber-Taper-Coupled Microresonator System for Application to Cavity Quantum Electrodynamics," Phys. Rev. Lett. **91**(4), 043902 (2003).
31. B. E. A. Saleh and M. C. Teich, *Fundamentals of Photonics*, Wiley Series in Pure and Applied Optics (John Wiley & Sons, Inc., 1991).
32. P. G. D. Gennes, F. Brochard-Wyart, and D. Quéré, *Capillarity and Wetting Phenomena : Drops, Bubbles, Pearls, Waves* (Springer, 2003).
33. C. F. Bohren and D. R. Huffman, *Absorption and Scattering of Light by Small Particles* (Wiley, 1998).

## 1. Introduction

As no liquid is perfectly transparent and non-scattering, it is natural to check if the transfer of momentum from light to liquid initiates flows. This way, light can act as a pump in almost any optofluidic system. Optofluidic resonators [1–4] are useful in detecting proteins [5], nanoparticles [6,7] and viruses [8]. Such microfluidic cavities were made in the form of a submerged solid-resonator [9], a solid resonator with liquid inside [10–12], or in the form of a droplet resonator [13–19]. A droplet is a small volume of self-contained liquid that is bounded almost completely by free surfaces. Its liquid-phase boundary typically self-forms to its final shape governed by interfacial tension. The droplet benefits from a nearly atomic-scale surface smoothness, which is necessary for reducing optical scattering-losses. A droplet can contain three types of resonances: optical, acoustic, and capillary. The optical modes of a droplet were recently mapped [20], and the droplets acoustic [21] and capillary modes [22,23] were optically excited.

Last and most relevant here, nanoparticles at the evanescent region of a submerged solid cavity were recently observed orbiting [24], locked to the evanescent tail of the mode. Such a whispering gallery mode (WGM) carousel [24] raises the question of whether optical momentum can similarly generate circulating flows in droplets. The circulating light contains angular momentum as explained in reference [25]. Interestingly, this angular momentum is taken from the fiber, similar to a steam-engine wheel taking linear momentum from the cylinder and turning it into angular momentum. As one can see in Fig. 1, microwatt-scale optical power is coupled into the circulating WGM of a droplet. When the pump laser is tuned via one of the droplet resonances, a dip in the optical transmission is measured, as shown in Fig. 2 inset. Let's assume that part of the optical losses in this resonator are due to absorption. Momentum conservation consideration implies that an absorbed power must apply azimuthal force on the liquid that is tangential to its equatorial line. Also relevant here is that in contrast to solids, where one has to overcome the static friction to start motion; liquid viscosity is typically speed independent. As a result, optically induced flows do not have an optical power threshold. Thus, there is no question if the light will initiate flow; the only question is what will be the speed of this flow. Surprisingly maybe, in a cavity where the major loss mechanism is absorption, the optically induced flows are independent of its optical quality factor. This is because it does not matter if an optical power will be absorbed after circulating

Optics EXPRESS

one round-trip or 1000 round-trips in the cavity. For in both cases a similar amount of momentum will be transferred to the microdroplet.

As for mapping the flows, we do so by inserting and mixing fluorescent nanoparticles in the liquid. As explained in the last section (Eqs. (4-7), we took special care in verifying that the nanoparticles are probing the flows while drifting at the speed of the liquid molecules.

Generally speaking, three loss mechanisms exist in the whispering gallery resonator: absorption, scattering and radiation. Leakage of light out of the cavity via radiation is negligible here, as calculated [26] and experimentally measured [27]. This is because the radius of our resonator is relatively large and the contrast between the refractive indices for the air clad and the liquid core is high. Thus, optical loss is governed by absorption, where each photon fully transfers its momentum to the medium and via backward scattering where each photon transfers twice its momentum.

Assuming that the optical losses in the cavity are by absorption, the optical force that pushes the liquid near the air-liquid interface to circulate is

$$F_0 = \frac{n \cdot P}{c}. \tag{1}$$

where P is the portion of input optical power that is absorbed by the cavity, c is the speed of light and n the refractive index of the droplet liquid. The drag forces, Fs, which act against the optical forces, is estimated using the shear-flow equation:

$$F_s = \mu A \frac{u}{y}, \tag{2}$$

where μ is the dynamic viscosity, u is to the speed of liquid at the air-liquid interface and y is the distance from the liquid-air interface to the stem at the region of motion. A is the area of the moving liquid at the liquid-air interface and is equal to the circumference of the droplet multiplied by the width of the optical mode along the stem. As mapped in [20], the width of the mode is typically 20% of the droplet extension along the stem.

After accelerating and then reaching steady state, the optical force [Eq. (1) is fully balanced by the drag force (Eq. (2)]. Using this relation, we can calculate the speed at the liquid-phase boundary:

$$u = \frac{yn}{\mu A c} P. \tag{3}$$

To give a relevant scale, a typical droplet might be 100 μm in diameter and the stem holding it might be 10 μm in diameter. The liquid can have a viscosity of 10 cSt, and a refractive index equals to 1.4. Coupling 4 microwatt of light to such a droplet will induce a 9.22 μm/s flow-speed according to Eq. (3). This estimation, in fact, implies that flows exist in almost any optofluidic resonator including the ones described in [1–24].

## 2. Experimental setup

We fabricate our droplet cavities by dipping a silica stem in silicone oils (Sigma-Aldrich #378321 or #378356). As a result of interfacial tension between the solid stem and the liquid, droplets tend to drift toward the thicker part of the stem to maximize the solid-liquid interface. Using this mechanism, we pin the droplet to the taper end by turning the solid stem-end into a small sphere, using a fiber splicer.

As one can see in Fig. 1, we use a tapered fiber to evanescently couple [28–30] a tunable laser (970 nm) into the droplet resonator. The standard coupling-mechanism here is based on the overlap between the resonator- and taper- modes, enabling light to pass from one to the other. This mechanism is described in more details in references [28–31].

Optics EXPRESS

The light transmitted through the droplet is coupled out through the other side of the taper and measured with a photodetector. A nanopositioning system is used to control the distance between the coupler and the resonator [Fig. 1(c)].

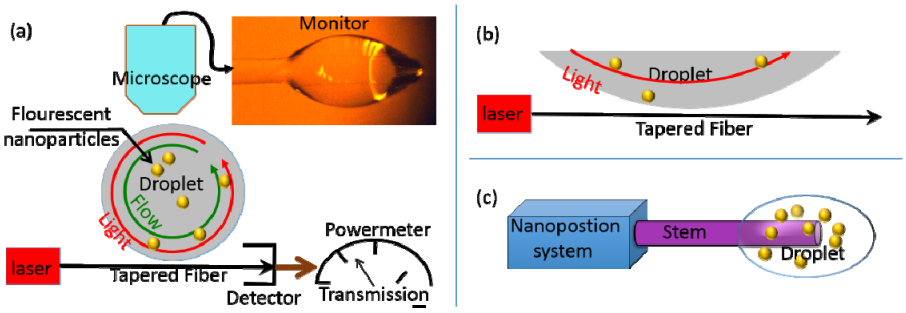


Fig. 1. Experimental setup for measuring light induced flows. (a) Circular flows (green) are excited by the droplets' optical-resonance (red). Streamlines are monitored by filming the tracks of fluorescent nanoparticles (yellow) while the optical resonances are excited using a tapered-fiber coupler. (b) Enlarged drawing of the coupling region where the typical gap between the taper and resonator is 500 nm. (c) The mechanism that holds and aligns the droplet resonator.

This optically-pumped droplet per se is sufficient for optically induced flows. However, in order to film these flows, we mix fluorescent polymer nanospheres (Bang FS02F envy green) in the liquid. We saw no buoyancy or sinking of the fluorescent nanoparticle. We film the nanoparticle's path which represents the flow streamline. Furthermore, when defocused, the microscope smears the nanoparticle's image into a larger spot. The position of the yellow fluorescent spot [Fig. 4(b)], together with its diameter [Fig. 4 (a-b)], allows us therefore to get its position in 3 dimensions.

For minimizing the optical forces on the nanoparticles probe, we use small nanoparticles with low absorption coefficient. The mean diameter of the nanospheres is 60 nm, and their refractive index is 1.57. The nanospheres are fluorescently excited by a green laser (532nm) and emit yellow light (565nm). Using a yellow-pass filter, we film the streamlines by tracking the nanoparticles.

## 3. Experimental results

In what follows, we parametrically study the optically induced flows while changing the optical input power, the resonator size and the viscosity of the liquid. As one can see in Fig. 2 (violet), increasing the input power from 0 to an estimated power of 4 μW, for a 10cSt-viscosity droplet with a diameter of 100 μm and a refractive index of 1.4 reveals a linear increase of the velocity from rest to 12.5 μm/s. Speed is measured here by monitoring the nanoparticle location vs. time. Such a linear behavior is expected from Eq. (3). We now repeat this experiment while changing the diameter of the droplet to 200 μm. As one can see in Fig. 2 (green), speed goes down with resonator size.

Optics EXPRESS

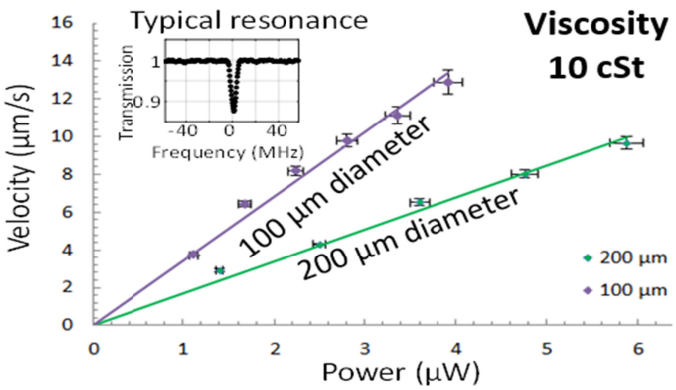


Fig. 2. Optically induced vortices are faster in small resonators. Flow speed as a function of the input optical power in droplets 10 cSt in kinematic viscosity and different diameters of 100µm and 200µm. The violet (green) curve is the fitted linear line to the measured speeds in the 100 µm (200 µm) with an R2 = 0.978 (0.981). The flow velocity was calculated by averaging three measurements, and the error bar of the velocity is the standard deviation. Inset: transmission dip at resonance, as measured by scanning the laser frequency though resonance while monitoring the output power (using the detector in Fig. 1).

Using Eq. (3), we can calculate that a rise of a droplet radius from 100 µm to 200 µm will reduce the speed by 2 (while the experimentally measured speed reduction is 1.97). We then repeat the experiment measuring the speed as a function of an input power, but this time at a higher viscosity as shown in Fig. 3. As expected from Eq. (3), increasing the viscosity indeed reduced the speed; yet, the exact amount of speed reduction is less than what is predicted by Eq. (3). This might be explained by the longer molecular chains of the high viscosity liquids. Such longer chains might scatter more light to enhance force.

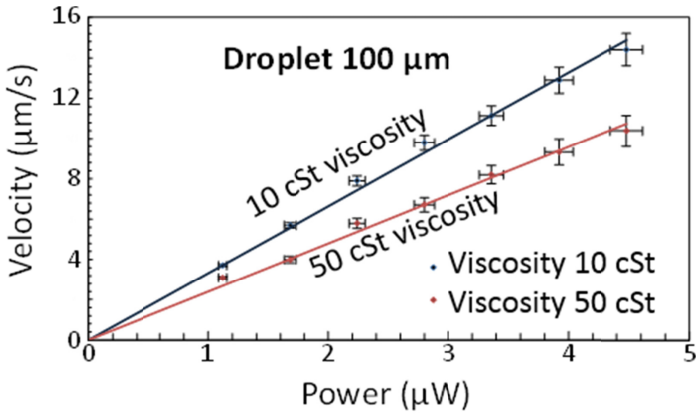


Fig. 3. Optically induced vortices slows down with viscosity. Flow speed as a function of optical power for droplets of two different viscosities. The blue (red) curve represents a linear fit to the measured velocity for a droplet having a 10 cSt (50 cSt) viscosity with an $R^2 = 0.992$ (0.988). The error bar was calculated as explained in Fig. 2 caption.

Optics EXPRESS

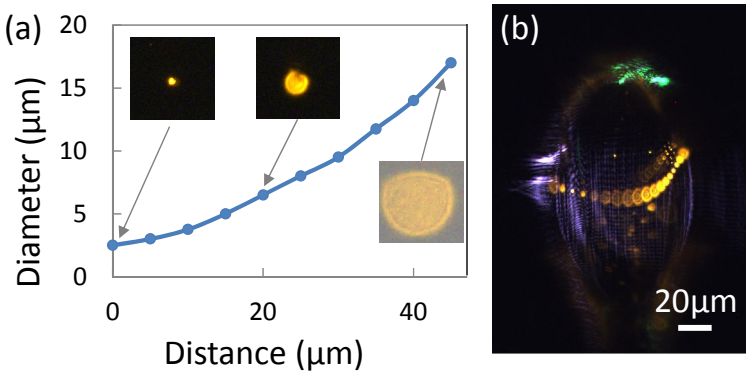


Fig. 4. (a) Calibration: the blue curve shows the fluorescent nanoparticle image diameter as a function of the distance along the optical axis of the microscope. (b) Merging of video frames showing the path of a nanosphere during half round in a droplet with a diameter of 100 μm presented in Visualization 1.

As one can see in Fig. 4(a), moving the particle toward the camera results in blurring. In order to get a lookup table of the nanoparticle distance to the microscope as a function of spot size; we take a coverslip, put on a fluorescent nanoparticle and captured a series of images while controlling the distance using an XYZ piezo stage. This measured relation between blurring and distance is presented in Fig. 4(a). We merge 18 frames from a movie of the flowing nanoparticle and present them in Fig. 4(b). As one can see [Fig. 4(b)], the position and blur of the 18 spots reveal the 3D position of the nanoparticle for each of the 18 measurements.

Using this method, we now map the nanoparticle trajectory in 3D. As one can see in Fig. 5, the streams are almost circular. This small droplet is axially symmetric since benefiting from a large surface tension to gravity ratio, as typical to small droplet [32].

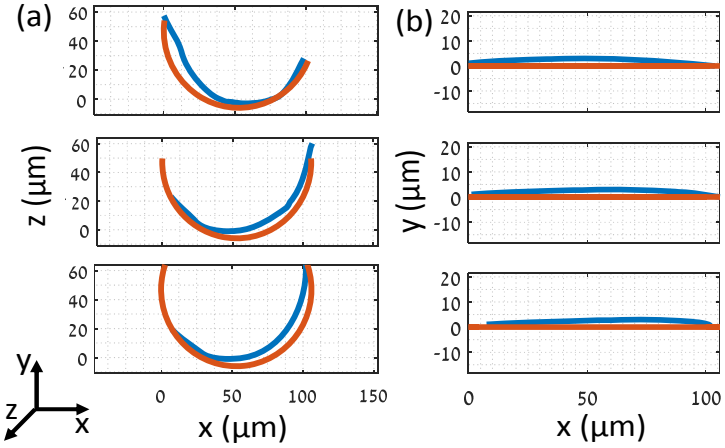


Fig. 5. 3D map of optically induced flows in a circular droplet exhibit a circular flow. Fluorescent particles path of three successive rounds in a silicone oil droplet with a diameter of 100μm form the video in Visualization 1. (a) XY plane for each rotation. (b) XZ plane for each rotation. The blue curve is the path of each lap, and the red line is a guide for the eye. Deviation of the droplet's equatorial-line shape from a circle is smaller than 0.5%.

In Fig. 6, we present instabilities observed in a droplet with a diameter of 250μm, where due to the gravity, there is a fall in the droplet symmetry and the flow is non-circular. The anchor of this droplet is 28 μm away from the center, and the deviation of the droplet from a circular shape is 3%.

Optics EXPRESS

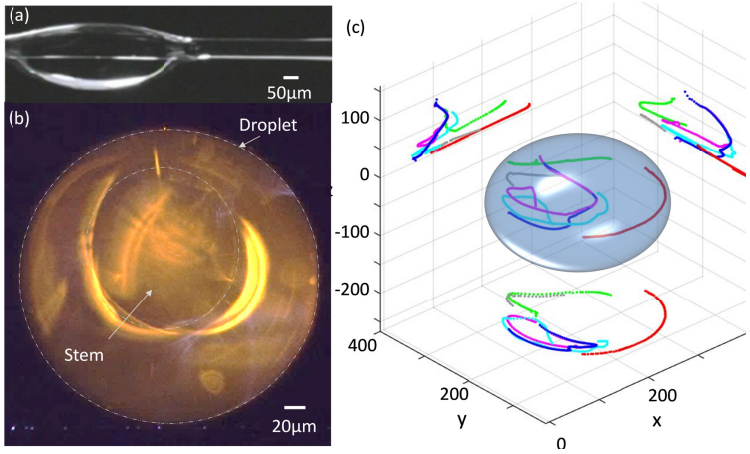


Fig. 6. 3D map of optically induced flows in a non-circular droplet exhibit non-circular flows (a) A micrograph of a silica micro stem holding a non-axially symmetric silicon oil droplet (b) A frame from a video (Visualization 2) showing the path of fluorescent nanospheres in a non-axially symmetric resonator. (c) Three dimension representation of droplet instabilities with a large diameter of 250μm. Each continuous line represents the path of a different fluorescent nanoparticle and accompanied by its projections on the XY, XZ and YZ planes.

As the nanoparticle functions here as a probe, it is important to show that the nanoparticle does not move with respect to the flow. We will start by calculating the force that light applies on the nanoparticle. Using the Rayleigh scattering equation, one can calculate the cross-section area for scattering, $\sigma_{sca}$ [33]:

$$\sigma_{sca} = \frac{2\lambda^2}{3\pi}\alpha^6\left|\frac{m^2-1}{m^2+2}\right|, \tag{4}$$

where $\alpha = \frac{2\pi r}{\lambda}$, $m = \frac{n}{n_1}$ $\lambda$ is the incident wavelength, $r$ is the radius of the nanosphere $n$ is the refractive index of the sphere and $n_1$ is the refractive index of the silicone oil respectively.

The particles within the optical mode volume will experience the strongest scattering forces. The intensity within the mode volume is:

$$I = \frac{F \cdot P}{A_m}, \tag{5}$$

where F is the optical finesse, P is the source power and $A_m$ is the mode area in a direction perpendicular to propagation. Taking the most pessimistic assumption that all scattering is in the backward direction we get the strongest force that light can apply on the nanoparticle:

$$F_{scat} = \frac{2 \cdot \sigma_{sca} \cdot I \cdot n_1}{c}. \tag{6}$$

Now if the particle is moving with respect to the liquid, it will experience a drag force:

$$F_d = 6\pi\mu r v, \tag{7}$$

where v is the particle speed relative to the surrounding medium.

Optics EXPRESS

Calculating the nanoparticle speed induced by scattering [using Eqs. (6-7)] reveals a speed 102 times slower than that reported here. Our conclusion is hence that the nanoparticle motion properly describes the flow. Additionally, to verify that the nano-particle is not moving with respect to the liquid, we were performing a control experiment where the pump light was turned off while we were monitoring the fluorescent nanoparticle dynamics. If moving in respect to the fluid, the nanoparticles are expected to experience a force according to Eq. (6). Using Newton's second law and Eq. (6), one can show that if moving in respect to the liquid, the particle will stop almost immediately (within $10^{-11}$ seconds). Experimentally, we see no immediate slowing of the nanoparticle; and therefore conclude that the nano-particle motion in respect with the liquid is negligible here. An additional source of error might be the Brownian motion of the nanoparticle. We were therefore performing a control-group experiment where the nanoparticles were monitored while the pump was off. The nanoparticle drift during the time of a typical measurement (such as in Figs. 4-6) was 3.1 μm, which is less than the thickness of the line in Figs. 5-6.

## 4. Conclusion

To conclude our measurements, we were examining optofluidic resonators with axial symmetry as well as resonators that are non-axially symmetric, which were accordingly hosting circular and non-circular flows. The flow speed increases with power and decreases with resonator size and with viscosity. Flows start even in high-viscosity (50 cSt), low-power (microWatt) systems making them therefore relevant to many optofluidic systems.

## Funding

Israel Center for Research Excellence ICore "Circle of Light" (1902/12); Israel Science Foundation (2013/15).